Virtual Flutter Flight Test of a Full Configuration Aircraft with Pylon/External Stores

Dong-Hyun Kim*
School of Mechanical and Aerospace Engineering (ReCAPT)
Gyeongsang National University (GSNU)
900 Gazwa-dong, Jinju, Kyungnam, Korea 660-701

Hyuk-Jun Kwon and In Lee*****
Department of Aerospace Engineering
Korea Advanced Institute of Science and Technology (KAIST)
373-1 Kusong-dong, Yusong-gu, Taejon, Korea 305-701

Seung-Kil Paek****
Korea Aerospace Industries, Ltd.
Sanam-myeon, Sacheon, Gyeongsangnam-do, Korea 664-942

Abstract

An advanced aeroelastic analysis using a computational structural dynamics (CSD), finite element method (FEM) and computational fluid dynamics (CFD) is presented in this paper. A general aeroelastic analysis system is originally developed and applied to realistic design problems in the transonic flow region, where strong shock wave interactions exist. The present computational approach is based on the modal-based coupled nonlinear analysis with the matched-point concept and adopts the high-speed parallel processing technique on the low-cost network based PC-clustered machines. It can give very accurate and useful engineering data on the structural dynamic design of advanced flight vehicles. For the nonlinear unsteady aerodynamics in high transonic flow region, Euler equations using the unstructured grid system have been applied to easily consider complex configurations. It is typically shown that the advanced numerical approach can give very realistic and practical results for design engineers and safe flight tests. One can find that the present study conducts a virtual flutter flight test which are usually very dangerous in reality.

Key Word : External Store, Flutter, Aeroelasticity, Virtual Test, Transonic, Parallel Processing, CSD, FEM, CFD, Euler, Unsteady Aerodynamics.

Introduction

Generic multi-purpose military aircrafts are usually carrying the several types of wing-mounted external stores. Furthermore, loading an external store including pylon connection part is the basic configuration of modern fighters. External stores can change the

* Assistant Professor
E-mail : dhk@gsnu.ac.kr, TEL : 055-751-6125, FAX : 055-755-2081
** Ph.D. Student
*** Professor
**** Researcher

aerodynamic and aeroelastic characteristics of wings because of their aerodynamic, inertial, and elastic coupling effect with the wing. The danger arises because the transonic regime is often the most critical from a structural dynamic stability. Nevertheless, the actual extent of the safety margins present in the design, such as the traditional flutter speed margin of 15~20% over a design dive-speed, cannot be demonstrated in flight test because of either safety or performance limitations. It is essential, therefore, that accurate analysis method, supported and verified by carefully conducting experimental procedures, forms the cornerstone of the structural dynamicists contribution to the process of designing an advanced aircraft. As these aspects, it is practically needed to develop a delicate computational analysis system based on the advanced and general technologies such as CFD/CSD/FEM and must be an essential and powerful tool to virtually simulate dangerous flutter phenomena. Some of the most difficult and dangerous problems in aircraft aeroelasticity arise in the transonic flight regime. The major analytical difficulty stems from the fact that the governing equations of transonic flow are inherently nonlinear, which has effectively precluded analytical solution by traditional approaches.

Recently, Melville [1] practically conducted a nonlinear aeroelastic simulation for F-16 fighter configuration in transonic flight. The inviscid parallelized Euler code based on the structured grid system was applied for numerical computations. This may be the first successful approach considering a full configuration aircraft in the world, however this paper didn't consider any local motion of control surface such as flaperon, rudder and taileron and external stores. Some of previous papers investigated the effect of external store on aeroelastic instability. Pollock et al. [2] presented the effect of slender store aerodynamics on wing-store flutter and the numerical method based on the doublet lattice method and wind-tunnel data correction. Triplett [3] conducted linear flutter analyses for F/A-18 wing with a tip store using doublet lattice method. Guruswamy et al. [4] developed a computational method based on the ATRAN3S code and examined the influence of a tip store on transonic aeroelastic stability. Recently, Gern and Librescu [5] have conducted efficiently the work on static and dynamic aeroelasticity of laminated composite wings carrying external stores. Various useful parametric studies have been shown using the efficient numerical methods. Also, Kim el al. [6-8] have been accurately investigated several store effects on unsteady aerodynamics and aeroelastic safety problems in transonic and supersonic flow regions. Nowadays, the accurate prediction of flutter boundary becomes a really important one to minimize the structural weight and to estimate its actual flight performance in the design process. We have successfully considered a full configuration aircraft carrying two-external stores with fines, and all local motion of control surfaces [8]. It seems till now that no research works could simultaneously consider all of these as far as we know. Authors proudly think that we made one breakthrough in the computational aeroelasticity fields and this kind of work is the first successful one in the world. In addition, large amount of computational results (although not presented here) related to this work have been used in the design of a realistic supersonic fighter (T-50, Golden Eagle) under developing in Korea.

Computational Aeroelastic Analysis

The governing aeroelastic equations of motion of a flexible wing are obtained by using the Rayleigh-Ritz method. In this method, the resulting aeroelastic displacement at any time can be expressed as a function of a finite set of selected modes. The general motion of the wing can be described by the separation of time and space variables as follows:

$$\begin{aligned} \{u(t)\} &= [\,\Psi_x(x,y,z)]\{q(t)\} \\ \{v(t)\} &= [\,\Psi_y(x,y,z)]\{q(t)\} \\ \{w(t)\} &= [\,\Psi_z(x,y,z)]\{q(t)\} \end{aligned} \tag{1}$$

where {u(t)}, {v(t)} and {w(t)} are the time-dependent structural deflections and $[\Psi_x]$, $[\Psi_y]$ and $[\Psi_z]$ are the matrices of x-, y- and z-direction displacements of the natural vibration modes. Usually, the number of column for the modal matrix $[\Psi]$ directly depends on the selection of the considering natural mode used in the coupled aeroelastic analysis.

The aeroelastic equations of motion for an elastic wing are formulated in terms of generalized displacement response vector {q(t)} which is a solution of the following equation:

$$[M_g]\{\ddot{q}(t)\}+[C_g]\{\dot{q}(t)\}+[K_g]\{q(t)\}=\{F_g(t, q, \dot{q})\} \tag{2}$$

where t is the physical time, $[M_g]$ is the generalized mass matrix, $[C_g]$ is the generalized damping matrix, $[K_g]$ is the generalized stiffness matrix, and $\{F_g\}$ is the vector of generalized aerodynamic forces computed by integrating the pressure distributions on the wing surface as

$$F_{gi}=\frac{1}{2}\rho U^2 c_r^2 \int\int_S -Cp(x, y, z, t)(n_x\Psi_{x_i}+n_y\Psi_{y_i}+n_z\Psi_{z_i})\frac{dS}{c_r^2} \tag{3}$$

where ρ is the free stream air density, U is the free stream velocity, c_r is the reference chord length, S is the wing area, C_p is the unsteady pressure coefficient on the arbitrary wing surface, n_x, n_y and n_z means the surface normal vectors for x, y and z direction, respectively and Ψ_i are the i-th natural mode shape vectors interpolated on the aerodynamic surface mesh. The generalized aerodynamic forces of Eq. (3) are integrated numerically on the wing, pylon, body and store surfaces. Unsteady Euler aerodynamic analysis based on the unstructured grid system [8] is coupled and used in this study.

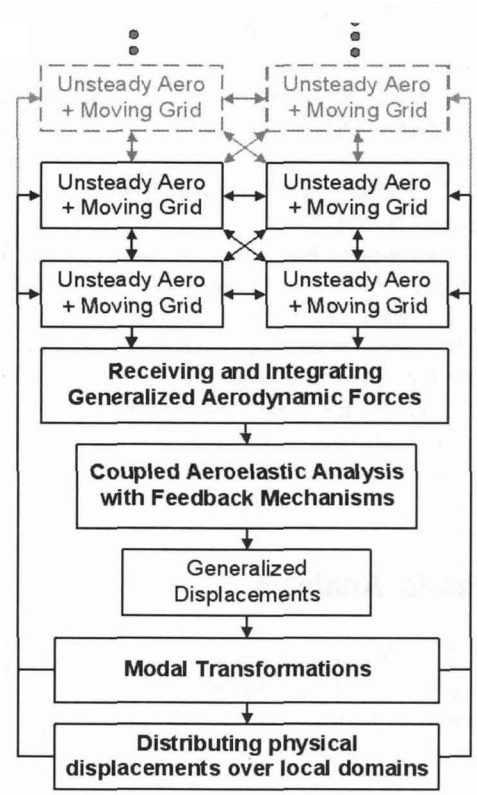

Fig. 1. Basic road map of a message passing concept on the coupled parallel aeroelastic analysis.

In general, the computation time needed in solving the structural equation is much less than those required in the decomposed fluid domains. Thus, to the parallel coupling with the unsteady fluid domains, one single computer node is usually prepared for solving the structural equations. At each global time step, all the local generalized forces computed from each computer node are to be transferred into the node for structure solver. Then, the generalized displacements can be obtained and the classified data for physical moving boundary are to be transferred into each corresponding computer nodes for spring analogy and unsteady fluid solution (Fig. 1). Data communications among computer nodes are also conducted using the standard message passing interface (MPI) library installed on a LINUX operating system. In addition, this includes the staggered coupling algorithm with internal iterations to increase the temporal coupling accuracy. In this study, the time marching process of the structure-fluid coupling was performed by similarly adopting the second-order staggered algorithm. It was known that this algorithm is constructed as a leap-frog scheme where the fluid subsystem is always computed at half time-stations, while the structure subsystem is always computed at full time-stations. The road map of the coupling process applied in this study is shown in Fig. 2.

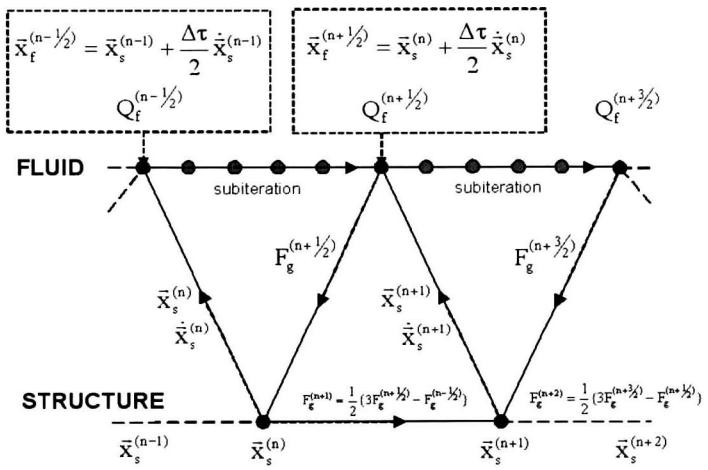

Fig. 2. Second-order time accurate staggered procedure.

Here, the transferred structural displacement and velocity are to be normalized to keep the numerical consistency with the normalized fluid domain.

Introducing the state vector {x} in order to efficiently perform the numerical integration, Eq. (2) can be recast into the first order form as

$$\{\dot{x}(t)\} = [A]\{x(t)\} + [B]\{\Gamma(t)\} \tag{4}$$

where

$$[A] = \begin{bmatrix} [0] & [I] \\ -[M_g]^{-1}[K_g] & -[M_g]^{-1}[C_g] \end{bmatrix}, \quad [B] = \begin{bmatrix} [0] \\ [M_g]^{-1} \end{bmatrix}$$

$$\{x(t)\} = \begin{Bmatrix} \{q(t)\} \\ \{\dot{q}(t)\} \end{Bmatrix}, \quad \{\Gamma(t)\} = \begin{Bmatrix} \{0\} \\ \{F_g(t)\} \end{Bmatrix}$$

Generally, to calculate the time response of Eq. (4) due to the initial condition, external forces or control inputs are needed to analyze the behavior of the system. For nonlinear structural systems, a typical numerical technique like Runge-Kutta method is commonly used and for linear structural systems we can use other approaches. One of the most useful and fast techniques for the linear system analysis can be derived from the assumption of setting the external force or control input constant, called zero order hold, during a certain small interval of time marching process.

Once the state transition matrix has been found, the solution to the homogeneous equation cab be determined. Taking the Laplace transform of Eq. (4) yields

$$s\{x(s)\} - x(0) = Ax(s) + B\Gamma(s) \tag{5}$$

solving for x(s) yields

$$\{x(s)\} = (sI - A)^{-1}x(0) + (sI - A)^{-1}B\Gamma(s) \tag{6}$$

or

$$\{x(s)\} = \Phi(s)\, x(0) + \Phi(s)\, B\Gamma(s)$$

$$\{x(t)\} = L^{-1}(sI - A)^{-1}x(0) + L^{-1}[(sI - A)^{-1}B\Gamma(s)] \tag{7}$$

Let's define the state transition matrix as

$$\{\Phi(t)\} = L^{-1}[(sI - A)^{-1}] \tag{8}$$

$$= L^{-1}\left[\frac{1}{(sI-A)}\right] = L^{-1}\left[\frac{\frac{1}{s}}{I-\frac{A}{s}}\right]$$

$$= L^{-1}\left[\frac{1}{s}\left\{I+\frac{A}{s}+\frac{A^2}{s^2}+\frac{A^3}{s^3}+\ldots\right\}\right]$$

$$= L^{-1}\left[\frac{I}{s}+\frac{A}{s^2}+\frac{A^2}{s^3}+\frac{A^3}{s^4}+\ldots\right]$$

$$= I+At+\frac{(At)^2}{2!}+\frac{(At)^3}{3!}+\ldots = e^{At}$$

Thus, we can obtain the following analytical form solution as

$$x(t) = e^{[A]t}\{x(0)\} + \int_0^t e^{[A](t-\tau)}[B]\{I(\tau)\}d\tau \tag{9}$$

The first term in Eq. (5) is the response due to the initial condition of the state and the second term is the response due to the forcing function. Also, the second term is considered as the convolution integral or Duhamel integral. The solution of Eq. (5) can be obtained numerically by replacing the continuous system by a discrete time system. A computational time interval Δt is considered so that $n\Delta t < t \leq (n+1)\Delta t$, and Eq. (9) can be written as

$$\{x(t)\}^{n+1} = e^{[A]\Delta t}\{x\}^n + e^{[A]\Delta t}\int_0^{\Delta t} e^{-[A]\tau}[B]\{I(\tau)\}d\tau \tag{10}$$

If we assume the generalized force is constant over the small time interval Δt then the integral can be evaluated.

$$\int_0^{\Delta t} e^{-[A]\tau}[B]\{I(\tau)\}d\tau = [A]^{-1}(I-e^{-[A]\Delta t})[B]\{I\}^n \tag{11}$$

Substituting the solution of the integral back into Eq. (10) yields

$$\{x\}^{n+1} = e^{[A]\Delta t}\{x\}^n + [A]^{-1}(e^{[A]\Delta t}-I)[B]\{I\}^n \tag{12}$$

From now on, Eq. (6) can be effectively integrated in time to predict the modal displacement and velocity using a digital computer as the following modified equation:

$$\{x\}^{n+1} = [\Phi]\{x\}^n + \frac{1}{2}[\Theta][B](3\{I\}^n - \{I\}^{n-1}) \tag{13}$$

where

$$[\Phi] = e^{[A]\Delta t}, \quad [\Theta] = [A]^{-1}(e^{[A]\Delta t} - I)$$

If the generalized mass, stiffness, and damping matrices are diagonal (proportional damping is practically assumed), the state matrix [A] can be expressed for each natural mode as the following decoupled form

$$[A]_i = \begin{bmatrix} 0 & 1 \\ -k_i/m_i & -c_i/m_i \end{bmatrix} = \begin{bmatrix} 0 & 1 \\ -\omega_i^2 & -2\zeta_i\omega_i \end{bmatrix} \tag{14}$$

where m_i, k_i, ω_i and ζ_i ($g_i \approx 2\zeta_i$) are the i-th generalized mass element, stiffness element, natural frequency and structural damping ratio, respectively. Thus, the analytical forms of the integration matrices Φ and Θ exist. So, for each degree of freedom, the state transition matrices can be expressed as

$$[\Phi] = \begin{bmatrix} \Phi_{11} & \Phi_{12} \\ \Phi_{21} & \Phi_{22} \end{bmatrix}, \quad [\Theta] = \begin{bmatrix} \Theta_{11} & \Theta_{12} \\ \Theta_{21} & \Theta_{22} \end{bmatrix} \tag{15}$$

where for each individual natural vibration mode the elements of state transition matrices are defined as follows:

$$\Phi_{11}=e^{a_i\Delta t}\left(\cos(b_i\Delta t)-\frac{a_i}{b_i}\sin(b_i\Delta t)\right),\quad \Phi_{12}=\frac{1}{b_i}e^{a_i\Delta t}\sin(b_i\Delta t)$$

$$\Phi_{21}=-\frac{a_i^2+b_i^2}{b_i}e^{a_i\Delta t}\sin(b_i\Delta t),\quad \Phi_{22}=e^{a_i\Delta t}\left(\frac{a_i}{b_i}\sin(b_i\Delta t)+\cos(b_i\Delta t)\right)$$

$$\Theta_{11}=\frac{1}{a_i^2+b_i^2}[2a_i(\Phi_{11}-1)-\Phi_{21}],\quad \Theta_{21}=\frac{1}{a_i^2+b_i^2}[2a_i\Phi_{12}-(\Phi_{22}-1)]$$

$$\Theta_{21}=\Phi_{11}-1,\quad \Theta_{22}=\Phi_{12}$$

where Δt is the numerical time step for the structural system, and coefficients a_i and b_i are defined as

$$a_i=-\zeta_i\omega_i,\quad b_i=\omega_i\sqrt{1-\zeta_i^2}$$

It may be noted that since the elements of the Φ and Θ matrices are dependent only on the values of time step size and ω_i, ζ_i which can be directly obtained from input matrices $[M_g]$, $[C_g]$ and $[K_g]$, so they need to be calculated only once at the beginning of aeroelastic computation. However, if the generalized mass, stiffness, and damping matrices are not diagonal, the analytical forms of the transition matrices are not available. In this case, Taylor series approximation of transition matrices may be used for actual numerical calculation or well-known numerical integration techniques such as Runge-Kutta (explicit) and Newmark (implicit) methods. The present aeroelastic analysis system can also select pure numerical time-integration solvers by changing an input parameter.

The computed natural vibration mode shapes are interpolated into the aerodynamic grid points using the surface spline methods. Unlike structured grid system, the unstructured aerodynamic grids automatically generated from a grid solver can hardly give ideally symmetric distributions on the object surface. In constructing the surface mesh, movable control surfaces such as flaperon, horizontal tail and rudder that may have independent and discontinuous motions need some artificial treatment to make independent surface splines and to increase the numerical stability. In this study, the artificial gaps are enforced on the boundaries where the discontinuities are typically expected. By applying the principle of virtual work, the relations between the finite element node and the aerodynamic grid points can be defined to interconnect each other. In this study, the numerical interpolations for the wing and pylon parts are carried out by infinite-plate spline (IPS) because of its numerical smoothness and robustness. For the external stores with fins, the method based on the generalized beam deflection theory is simply used because of its axisymmetric shape. As mentioned before the store is assumed as a nearly rigid beam structure with concentrated mass located at c.g. point. This is straightforward and practical because the actual relative stiffness of store is very high compared with those of the wing and pylon structures. For the full configuration aircraft, thin-plate spline (TPS) technique is adopted to interpolate the horizontal tail because of its anhedral angle. In addition, applying a superposition technique with or without overlapping regions is basically useful in considering the complex shapes of flight vehicle structures that can be also decomposed as multi-components. Enforcing the overlapping region can increase continuity at the decomposed structural boundaries. After performing surface splines for each structural component, these can be simply assembled into the original global configuration. The global natural vibration mode shapes interpolated on the surface mesh of aerodynamic grid can be effectively displayed by the post-combination process using a general plotting program such as Tecplot. Recent useful information for several spline techniques with numerical experiments could be found from Ref. 9.

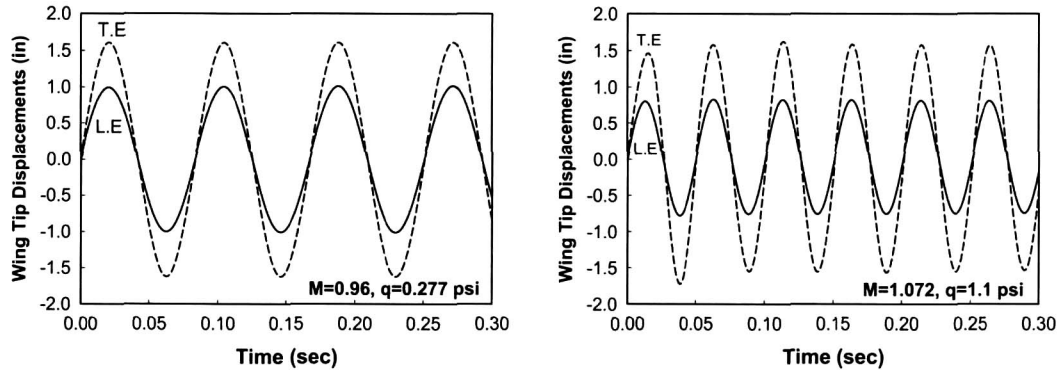

Fig. 3. Dynamic aeroelastic responses of AGARD 45-deg sweptback wing (M=0.96 and M=1.072).

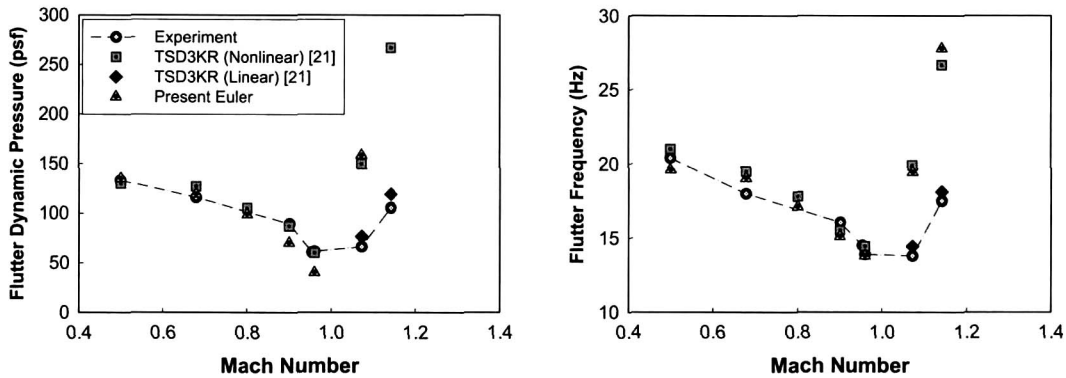

Fig. 4. Comparison of flutter dynamic pressure and frequency for the AGARD wing.

Results and Discussion

As the numerical validation of present computational aeroelastic analysis system, a well-known benchmark wing model named as AGARD standard aeroelastic configuration (weakened 445.6 model) has been analyzed. This series of wings was tested in the Transonic Dynamics Tunnel (TDT) at NASA Langley Research Center [10]. The wing has a NACA 65A004 airfoil section, a quarter-chord sweep angle of 45-deg (leading edge sweep of 46.3-deg), an aspect ratio of 3.3, and a taper ratio of 0.66. A matched-point flutter analysis was conducted for several Mach numbers. Each time-integration calculation was restarted from the steady-state solution, and the motion of the wing was initiated by specifying an initial modal displacement for the first mode. The damping ratio for each aeroelastic response was calculated using moving block (MB) numerical technique. The computed flutter dynamic pressures and frequencies were firstly predicted by interpolating the specified dynamic pressures to give the zero damping value of aeroelastic responses. Then, the flutter analysis was generally conducted to reconfirm the neutral stability of the predicted flutter dynamic pressure. Figure 3 shows physical aeroelastic responses at the wing tip which found as the neutral stability at M=0.96 and M=1.072. All the computations were effectively conducted on the PC clustered parallel machine. The computed flutter dynamic pressures and frequencies are compared with the wind-tunnel experimental data and the results are presented in Fig. 4. It shows good agreement with the experimental data for the transonic region.

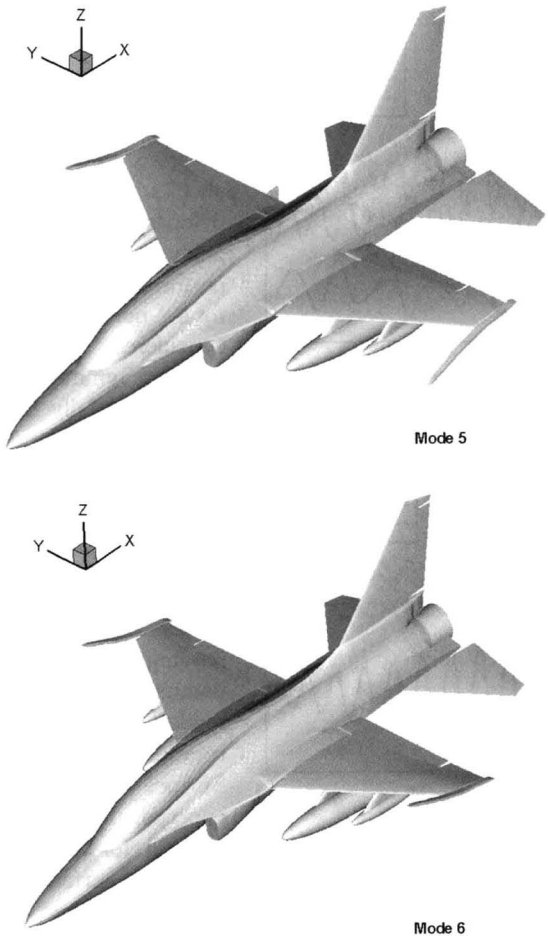

Fig. 5. Sample plots for the surface splined natural vibration modes.

A full configuration aircraft with a tip launcher and carrying two-external stores is considered in order to demonstrate a highly practical application. In addition, all local motions of control surfaces were simultaneously considered in this study. Because of the complex model geometry and control surface motion, lots of care have to be given in the initial grid generation process. Unstructured surface meshes for the present fighter model is generated using the GAMBIT grid generation software. The full grid domain consists of 554,295 tetrahedral cells and 115,446 nodes including the both aircraft sides. This grid size can be considered as really effective one even though it has enough grid resolution on the surfaces. The key point for reducing the overall grid size is to control the space resolution from the surface to the far field. Several techniques can be applicable to reduce the total grid number. If we use GUI based program such as GAMBIT to generate the complex unstructured grid system, it may be simply conducted and controlled graphically using the multi-overlapping concept about far domains. In constructing the surface mesh, moving control surfaces such as flaperon, horizontal tail and rudder can have discontinuous motions. Thus, some know-how such as using a artificial gap technique is needed. This is very important to keep the numerical robustness of aeroelastic solver and get successful computational results. Simultaneously, one also have to consider the grid skewness near surface and control surface boundaries. Actually, obtaining a converged steady aerodynamic solution is not a big problem even for the present aircraft model. One must have, however, several numerical instabilities for

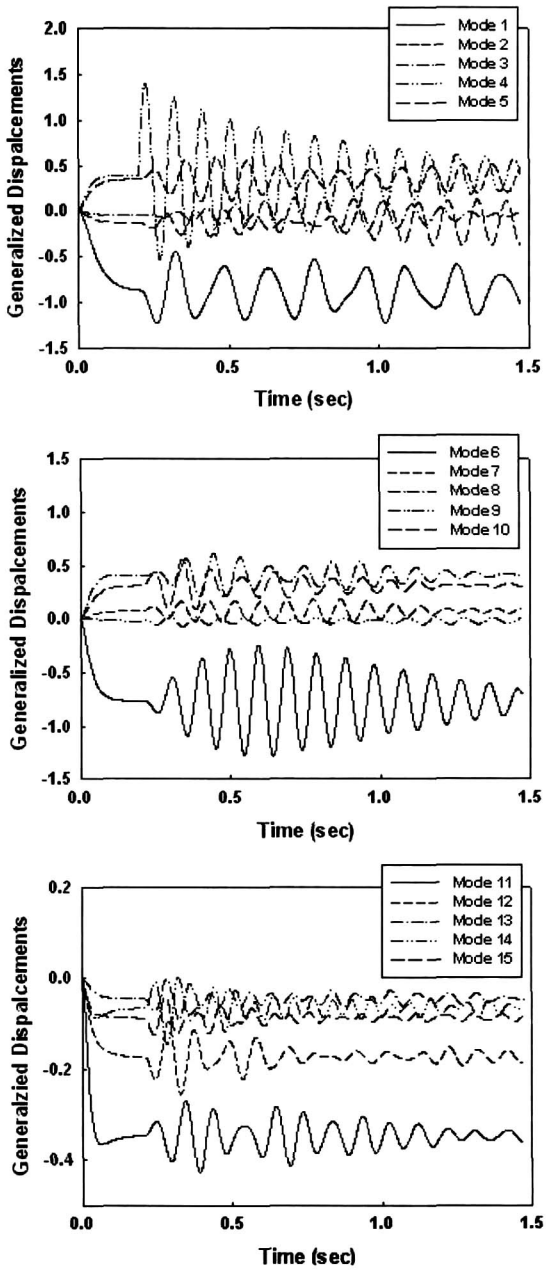

Fig. 6. Aeroelastic modal responses of the full configuration aircraft with a tip-launcher and two under-stores at M=0.9.

unsteady problems because of considering critical local rigid and elastic motions of boundary surfaces. The present store configuration does not allow the supersonic flight because of its military purposes. Complex flow interactions with normal shocks are expected in the vicinity of pylon/store locations. Dynamic structural analysis of the full aircraft model was also performed by the MSC/NASTRAN. The total number of free vibration mode considered here is twenty-five for this case. Symmetric and anti-symmetric modes are fully included except for the six rigid vibration modes. As an example of the superposed surface splines technique, two interpolated natural vibration modes are presented in Fig. 5. As shown in the figure, mode 5 is not a symmetric and contains the anti-symmetric wing tip launcher mode. The independent motions of moving control surfaces seem to be not dominant for this case. The other natural modes that are not presented here contain rotation displacements of control surfaces. Surface spline process even based on superposition concept is to be relatively difficult for this kind of complex geometry. Various surface spline techniques were tested, and then numerical robustness and accuracy were also compared to each other. It is experienced that a hybrid application of BS, IPS and TPS methods is very good and practical.

As the numerical demonstration of a really complex aeroelastic problem, some computational results are presented for a typical transonic flight condition. The flow condition is M=0.9 at α=0 deg. Figure 6 shows the modal transient responses of the present aircraft model. It shows that most of the modal responses are stable. Among them some critical damping can be observed at the fifth mode. Figure 7 shows the physical responses at several structural positions of the aircraft such as launcher noses, wing tips, flaperon trailing edges, store noses, horizontal tails, vertical tail and rudder trailing edge. In the present analysis, a user can specify desired structural locations to monitor the physical responses. Furthermore, user can make movie files for global flutter vibration phenomena which can be used as virtual flutter flight test data. In the figure, many of the responses also show the global stable damping ratios. However, we may see some small amplitude LCO responses at the wing tip trailing edge, the right inboard store and the right horizontal tail. The computed responses are

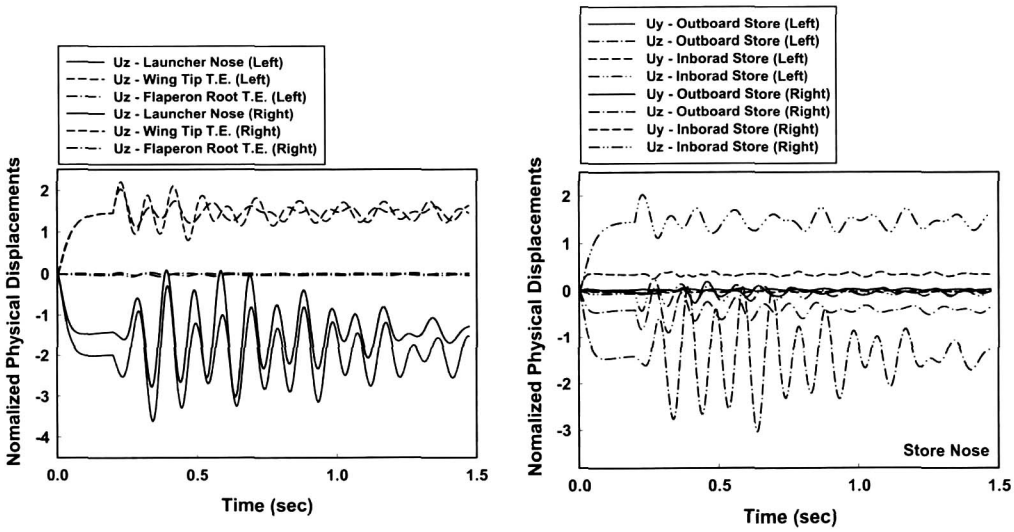

Fig. 7. Normalized aeroelastic responses of the full configuration aircraft with a tip-launcher and two under-stores at M=0.9.

not symmetric for the right and the left side since the full natural vibration modes are used in this study. Also, store aeroelastic vibrations are much more unstable on the right side wing and especially on the right-side outboard store. The low damping characteristics at some structural locations seem to be closely related with the unstable store vibrations and transonic shock waves. Thus, those must be carefully investigated in the actual design process since it can lead to critical and complex LCO phenomena in the normal flight conditions.

Conclusion

In this paper, a general aeroelastic analysis system coupled with advanced numerical methods such as CFD, CSD and FEM has been developed using high-speed parallel processing techniques. The application and robust numerical computations using the unstructured grid system have been conducted for highly complex configurations. A matched-point concept using standard atmosphere is applied to give physically meaningful flutter solutions on actual flight conditions of a aircraft. Using the developed analysis system, nonlinear dynamic aeroelastic behaviors of a full configuration aircraft carrying two-external stores were simulated in the transonic flow region. Also, all local motions of control surfaces were simultaneously considered. This practically indicates that present study virtually conducted aeroelastic flight tests which are usually very dangerous in reality. It was shown that the advanced numerical approach can give very practical information on flutter and aeroelastic responses of a designed aircraft before conducting dangerous flight tests to the transonic flutter. Successful applications for a really complex configuration show great potential for various practical applications.

Acknowledgement

This work was supported through funding from the National Research Laboratory (NRL) program (2000-N-NL-01-C250) of Korea Ministry of Science and Technology, the Research Center for Aircraft Part Technology (ReCAPT) of Gyeongsang National University (GSNU) and also by the research project with Korea Aerospace Industry (KAI). The authors would also like to acknowledge the supports.

References

1. Melville, R., "Nonlinear Simulation of F-16 Aeroelastic Instability," AIAA Paper 2001-0570.

2. Pollock, S. J., Sotomayer, W. A., Huttsell, L. J., and Cooley, D. E., "Evaluation of Methods for Prediction and Prevention of Wing/Store Flutter," *Journal of Aircraft*, Vol. 19, No. 6, June 1982, pp. 492-498.

3. Triplett, W. E., "Wind Tunnel Correlation Study of Aerodynamic Modeling for F/A-18 Wing-Store Tip-Missile Flutter," *Journal of Aircraft*, Vol. 21, No. 5, May 1984, pp. 329-334.

4. Guruswamy, G. P., Goorjian, P. M., and Tu, E. L., "Transonic Aeroelasticity of Wings with Tip Stores," AIAA Paper 86-1007, pp. 672-682.

5. Gern, F. H., and Librescu, L., "Static and Dynamic Aeroelasticity Wings Carrying External Stores," *AIAA Journal*, Vol. 36, No. 7, July 1998, pp.1121-1129.

6. Kim, D. H., and Lee, I., "Transonic and Low-Supersonic Aerodynamic Analysis of a Wing with Underpylon/Store," *Journal of Aircraft*, Vol. 37, No. 1, January-February 2000, pp. 189-192.

7. Kim, D. H., and Lee, I., "Transonic and Supersonic Flutter Characteristics of a Wing-Box Model with Tip Stores," AIAA Paper 2001-1464.

8. Kim, D. H., Park, Y. M., Lee, I. and Kwon, O. J., "Nonlinear Aeroelastic Computation of Wings with Pylon/Finned-Store Using Parallel Unstructured Euler Solver," AIAA Paper 2002-1289.

9. Smith, M. J., Cesnik C. E. S., Hodges, D. H., and Moran, K. J., "An Evaluation of Computational Algorithms to Interface between CFD and CSD Methodologies," AIAA Paper 96-1400-CP, pp. 745-754.

10. Yates, E. C., Jr., "AGARD Standard Aeroelastic Configurations for Dynamic Response. Candidate Configuration I:-Wing 445.6," NASA TM 100492, August 1987.